



Multiple observations and modeling of the tiny ground motions associated with coseismic gravity changes

Martin Vallée and **Kévin Juhel**

With inputs from Jean Paul Ampuero, Olivier Coutant, Robert Busby, Kasey Aderhold,
Jean-Paul Montagner...

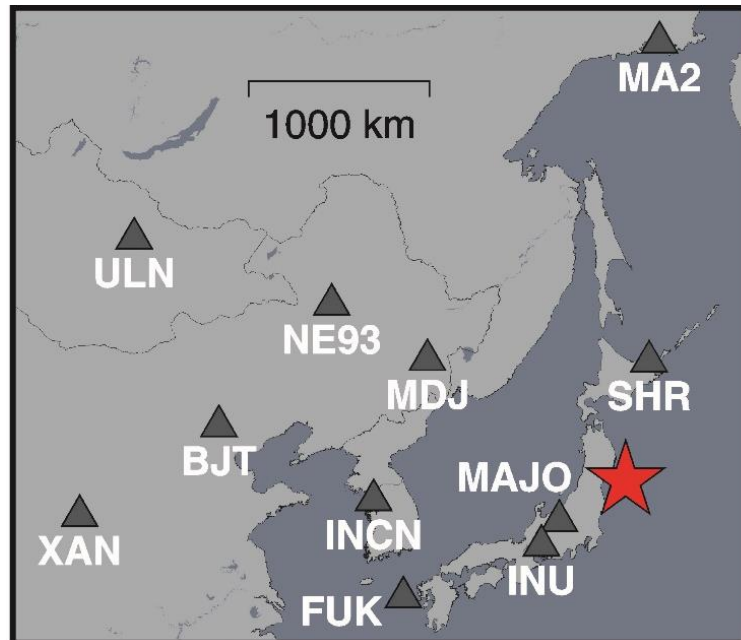
Extensive use of **publicly available broadband networks**

Numerical modeling of earthquake motions – Smolenice – July 3, 2019

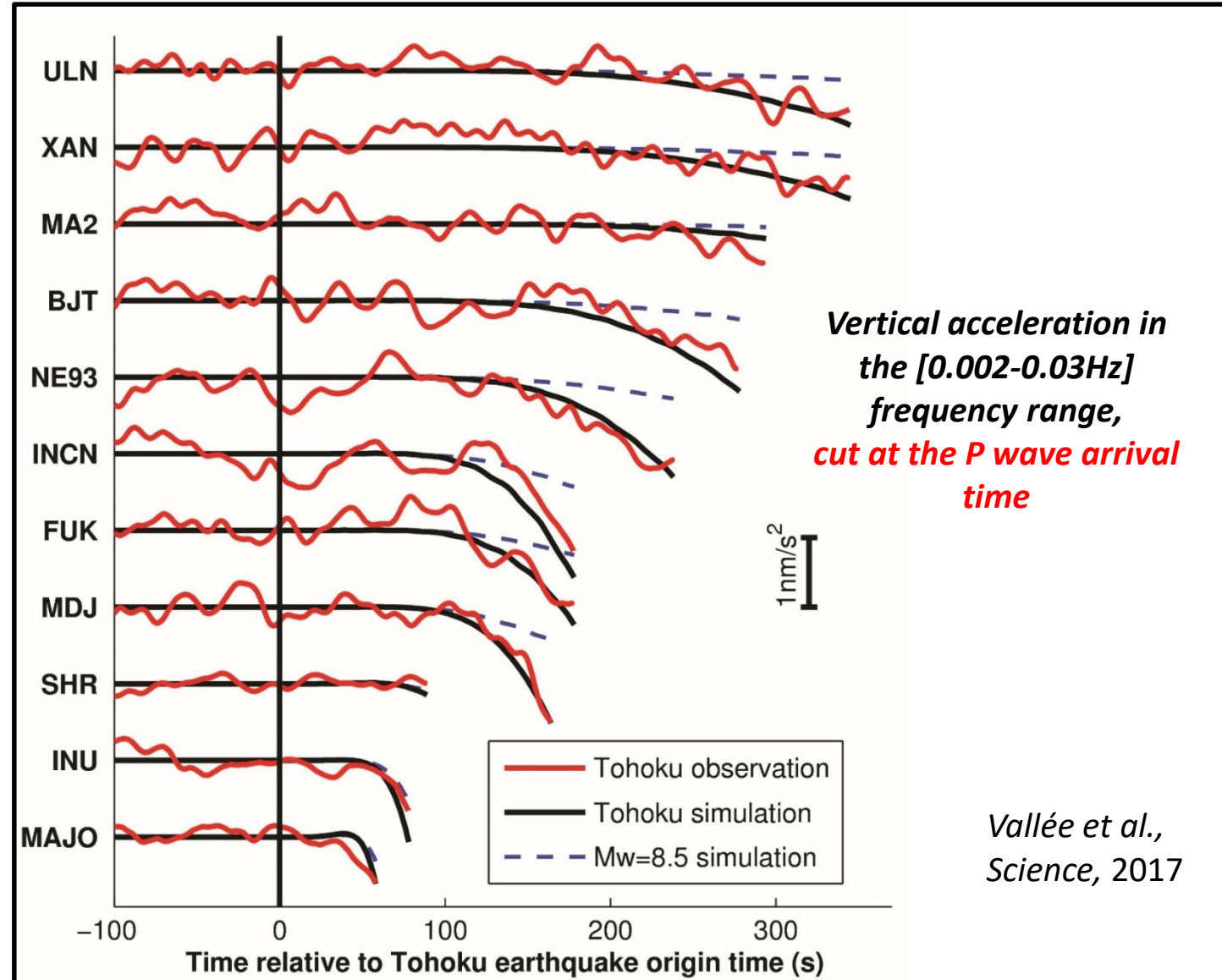
The Prompt Elastogravity Signals (PEGS)

- Use of an **unexploited** part of the seismograms : the time window **between origin time and P-wave arrival**
- High potential for **rapid determination of large earthquake source parameters**

First observed during the 2011 Mw=9.1 Tohoku earthquake [Montagner et al., 2016; Vallée et al, 2017]



At high-quality broadband stations, the PEGS are observed, modeled, and their amplitudes are strongly magnitude-dependent



How do we understand and model the Prompt Elastogravity Signals ?

$$\left\{ \begin{array}{l} \rho_0 \ddot{\mathbf{u}} = \nabla \cdot \boldsymbol{\sigma} + \Delta\rho \mathbf{g}_0 + \mathbf{f} + \rho_0 \Delta\mathbf{g}, \quad \text{Force balance equation (earthquake source term } \mathbf{f}) \\ \nabla \cdot \Delta\mathbf{g} = -4\pi G \Delta\rho, \quad \text{Poisson equation} \\ \Delta\rho = -\nabla \cdot (\rho_0 \mathbf{u}), \quad \text{Continuity equation} \end{array} \right.$$

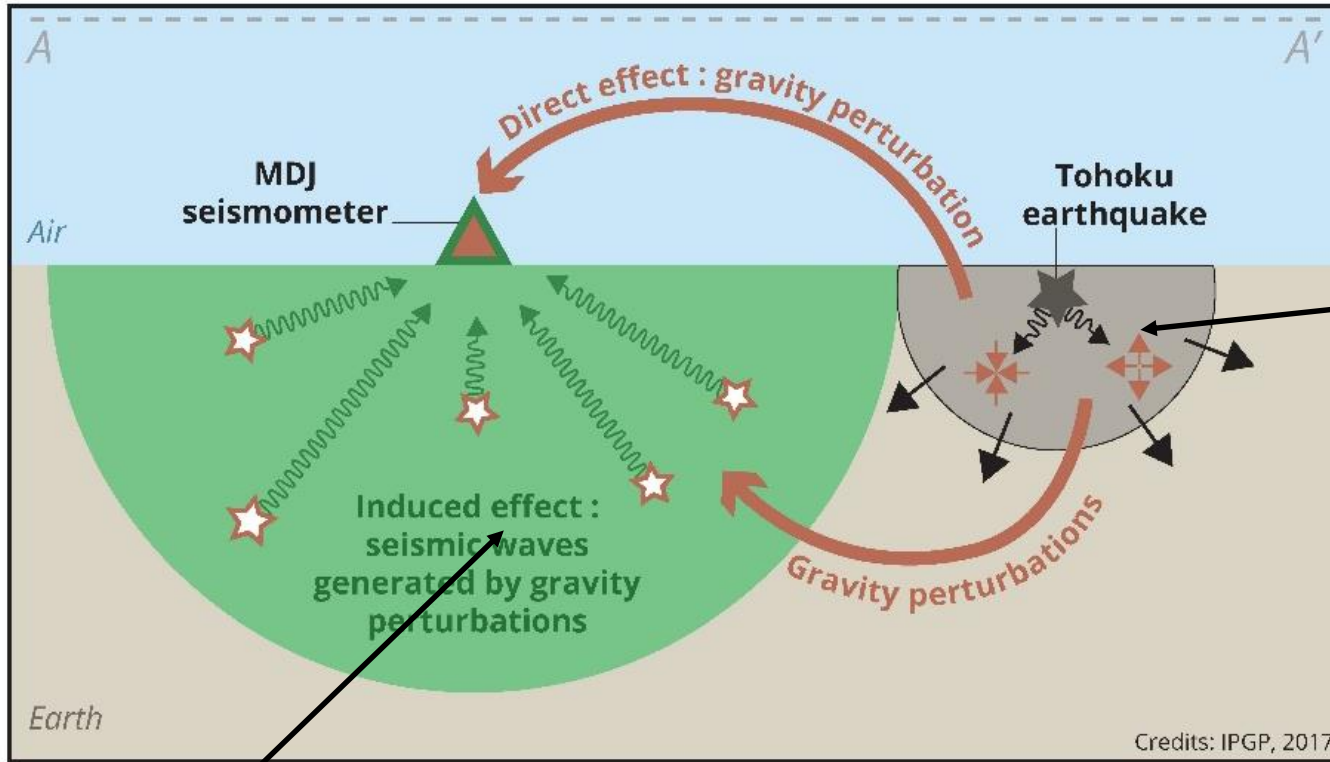
 In theory, there is a **full coupling** between the gravitation perturbation $\Delta\mathbf{g}$ and the displacement \mathbf{u}

However, for the force balance equation :

(1) **Close from the source** (i.e. at locations where P waves already arrived), and at not-too-low frequencies (above $\sim 0.001\text{Hz}$), the source term \mathbf{f} largely dominates over the force gravity terms

(2) **Far from the source** (i.e. where P waves did not arrive yet), the source term \mathbf{f} has no direct influence and the density perturbation can be neglected : the only force term is $\rho_0 \Delta\mathbf{g}$

Illustration at some time between origin time and P-wave arrival



In the volume directly affected by the elastic waves (grey area) :

$$\rho_0 \ddot{\mathbf{u}} = \nabla \cdot \boldsymbol{\sigma} + \Delta\rho \cancel{\mathbf{g}_0} + \mathbf{f} + \rho_0 \cancel{\Delta\mathbf{g}},$$

\mathbf{u} can be known everywhere with numerical methods solving the classical elastodynamic equation (e.g. Axitra) with source term \mathbf{f} (earthquake)



This creates a gravity perturbation everywhere

$$\begin{cases} \nabla \cdot \Delta\mathbf{g} = -4\pi G \Delta\rho, \\ \Delta\rho = -\nabla \cdot (\rho_0 \mathbf{u}), \end{cases}$$

$\Delta\mathbf{g}$ can be known everywhere using an integral form of the Poisson equation (e.g. Dahlen & Tromp, 1998)

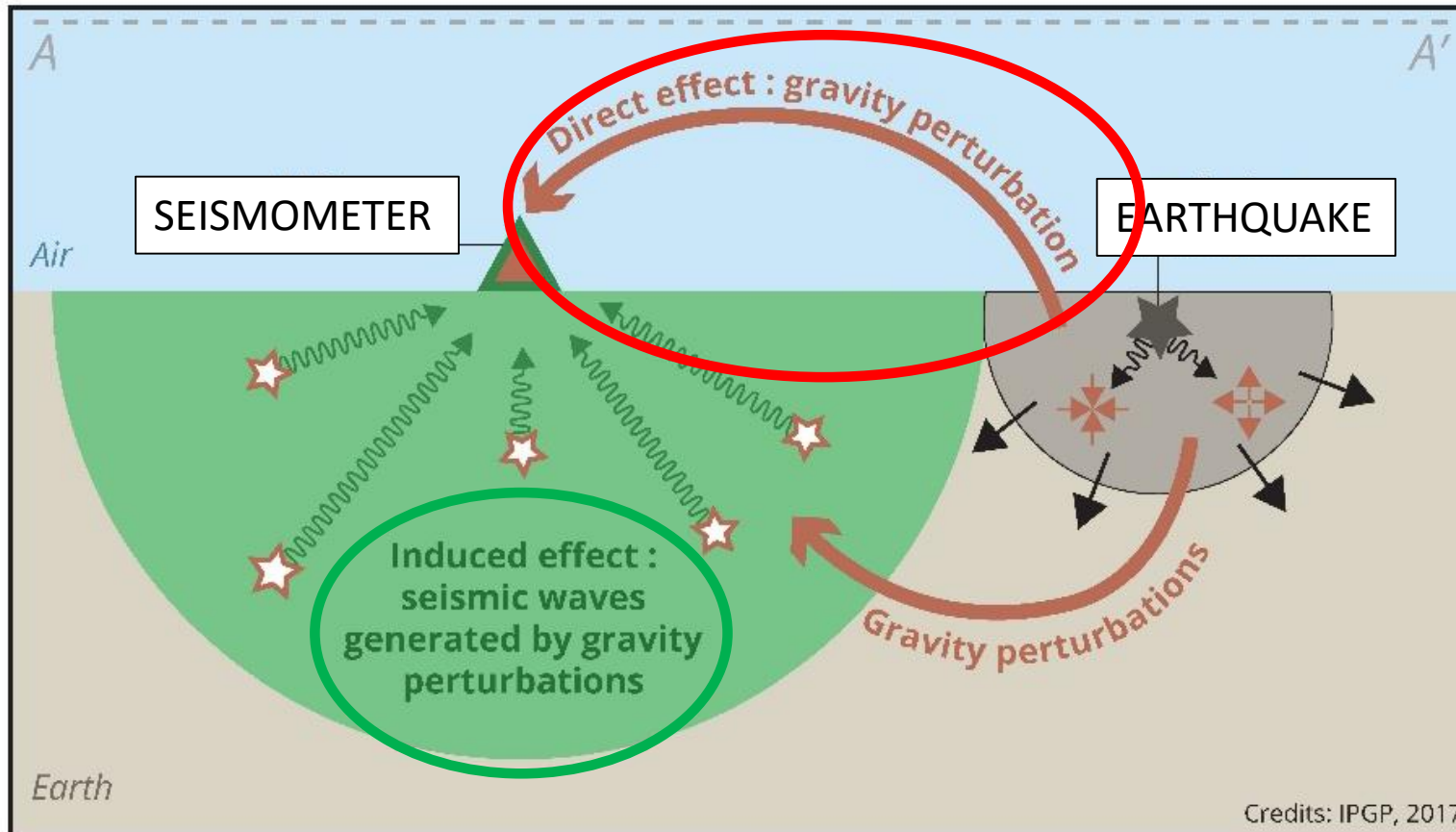
In the volume directly where gravity-induced elastic waves can arrive before the direct waves (green area)

$$\rho_0 \ddot{\mathbf{u}} = \nabla \cdot \boldsymbol{\sigma} + \Delta\rho \cancel{\mathbf{g}_0} + \cancel{\mathbf{f}} + \rho_0 \Delta\mathbf{g},$$

\mathbf{u} can be known everywhere with numerical methods solving the classical elastodynamic equation (e.g. Axitra), with source term $\rho_0 \Delta\mathbf{g}$



How do we understand and model the Prompt Elastogravity Signals ?



Schematic representation at a time between earthquake origin and P-wave direct arrival (direct elastic waves are inside the grey area)

As soon as an earthquake occurs (and **thus before the arrival of seismic waves**), a weak signal is expected to be recorded at a broadband seismometer, due to the **difference between** :

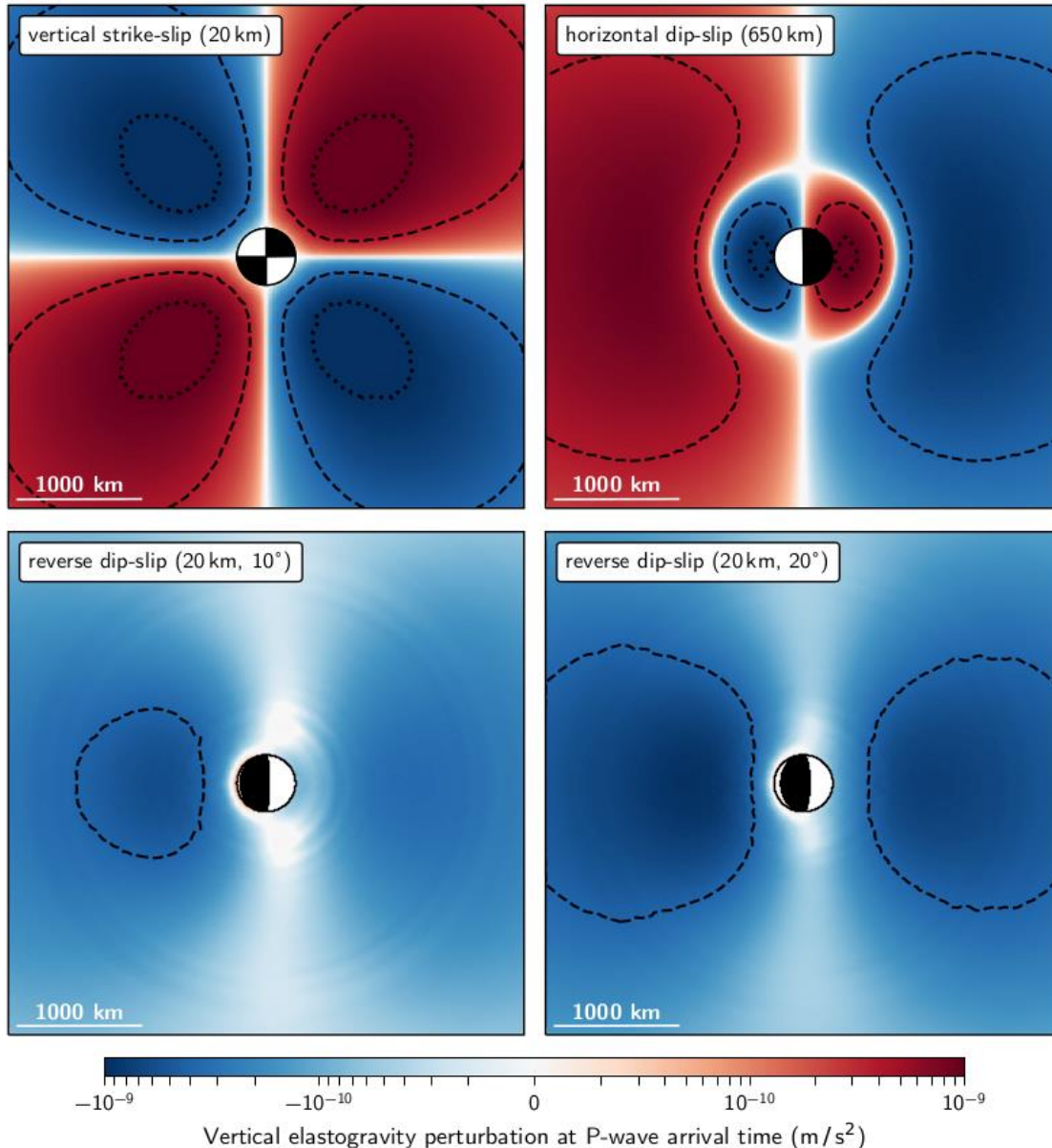
- The **gravity perturbation** induced by the earthquake rupture and elastic waves [Harms et al., 2015, Montagner et al., 2016] :
Direct effect
- The **elastic relaxation** of the Earth, itself affected by the gravity perturbations [Vallée et al., 2017, Juhel et al., 2018] :
Induced effect

« **Prompt Elastogravity signals** »

- **Questions following the first PEGS observations** made during the 2011 Tohoku earthquake, in order to **better assess the PEGS potential** for source parameter determination :
 - **What are the factors (other than magnitude) controlling the signal amplitude and detectability ?**
 - **Are such signals detectable for lower magnitude earthquakes ?**
 - **How can networks of broadband stations improve the signal detectability?**

Factors controlling the PEGS detectability

Mw=8.5 scenarios

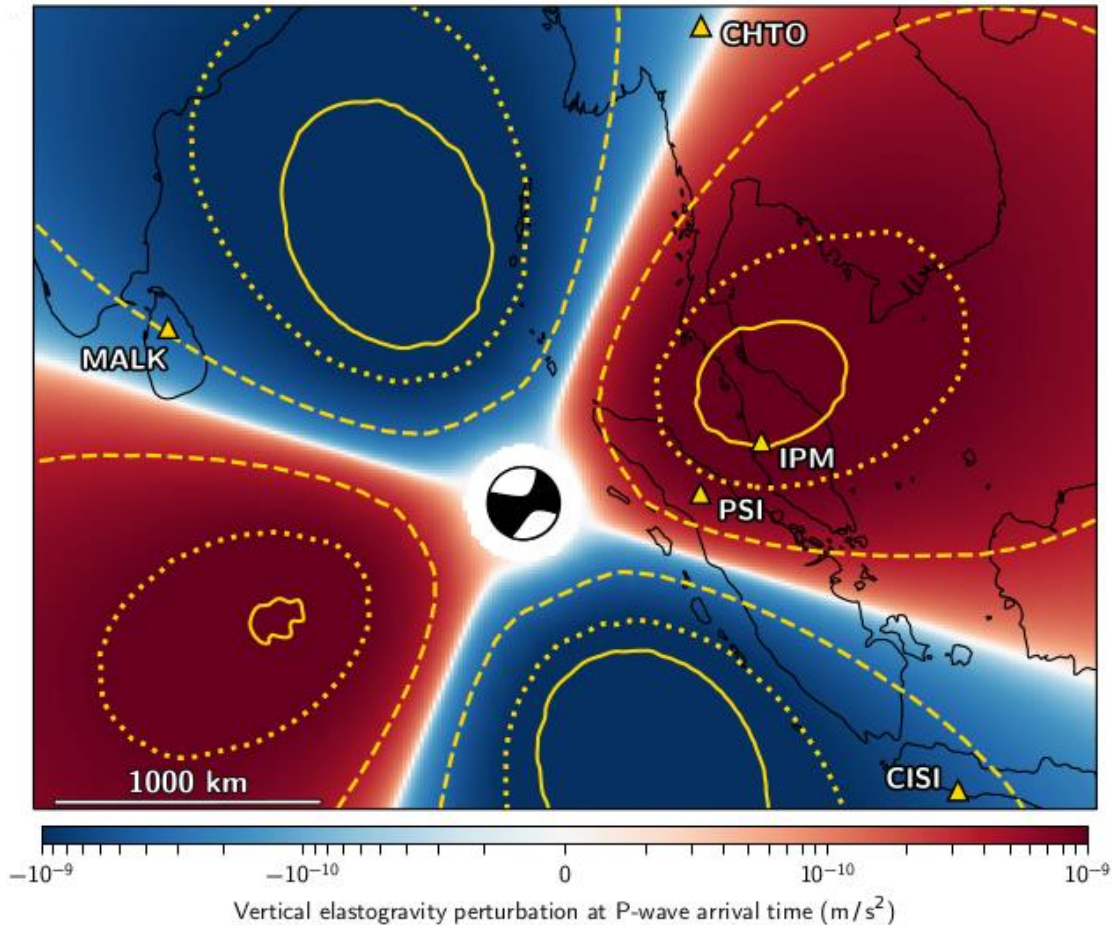


- 1) For a given magnitude and source time function (STF), **strike-slip and deep earthquakes generate larger PEGS than thrust earthquakes** on shallow dipping interfaces
- 2) Direct relation between STF and gravity perturbations [Harms et al., 2015] : **Rapidly growing moment rate functions increase the signal observability**
- 3) PEGS detection **requires the earthquakes to be recorded by good broadband stations in a relatively quiet seismic period** (e.g. not in the hours following a large earthquake)
- 4) For earthquakes generating PEGS close to the seismic noise, **detection can be achieved by combining the observations at several sensors** (array techniques)

Single-stations observations

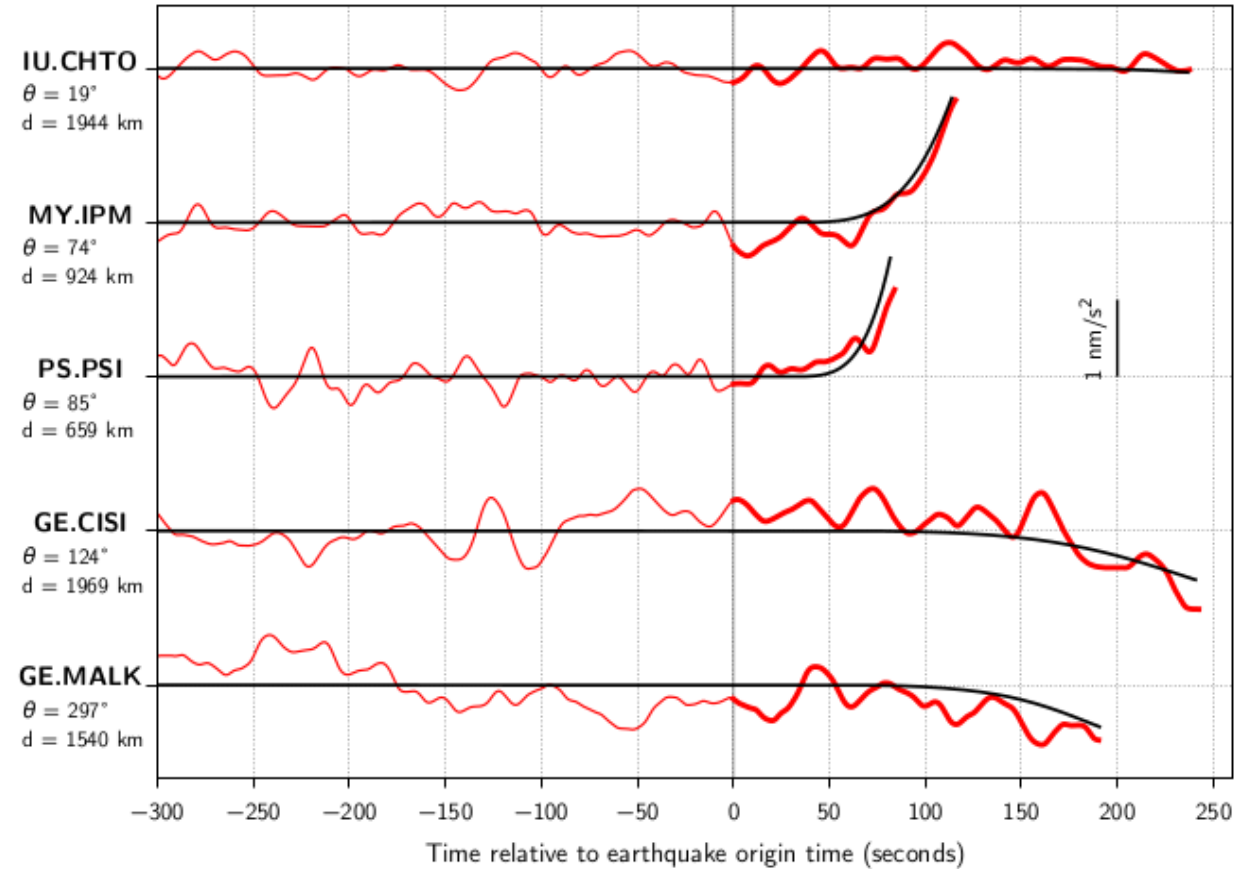
The 2012/04/11 Mw=8.6 Wharton Basin earthquake

Map showing the PEGS predicted amplitude (using GCMT source parameters), and the 5 broadband stations with lowest noise in the [0.002-0.03Hz] frequency range



Vallée and Juhel, 2019

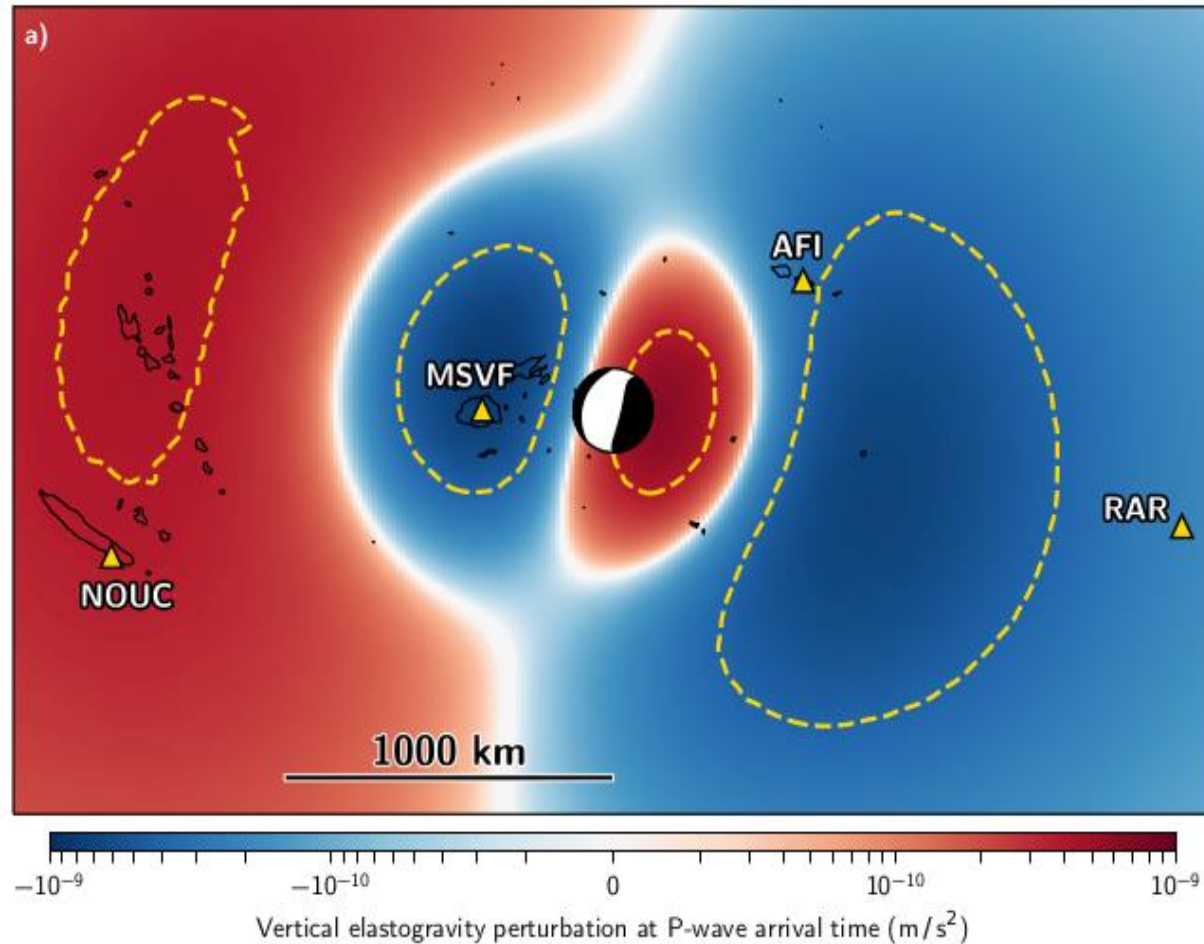
Observed (red) and modeled (black) waveforms at the 5 best stations, using an event-specific source time function (SCARDEC method)



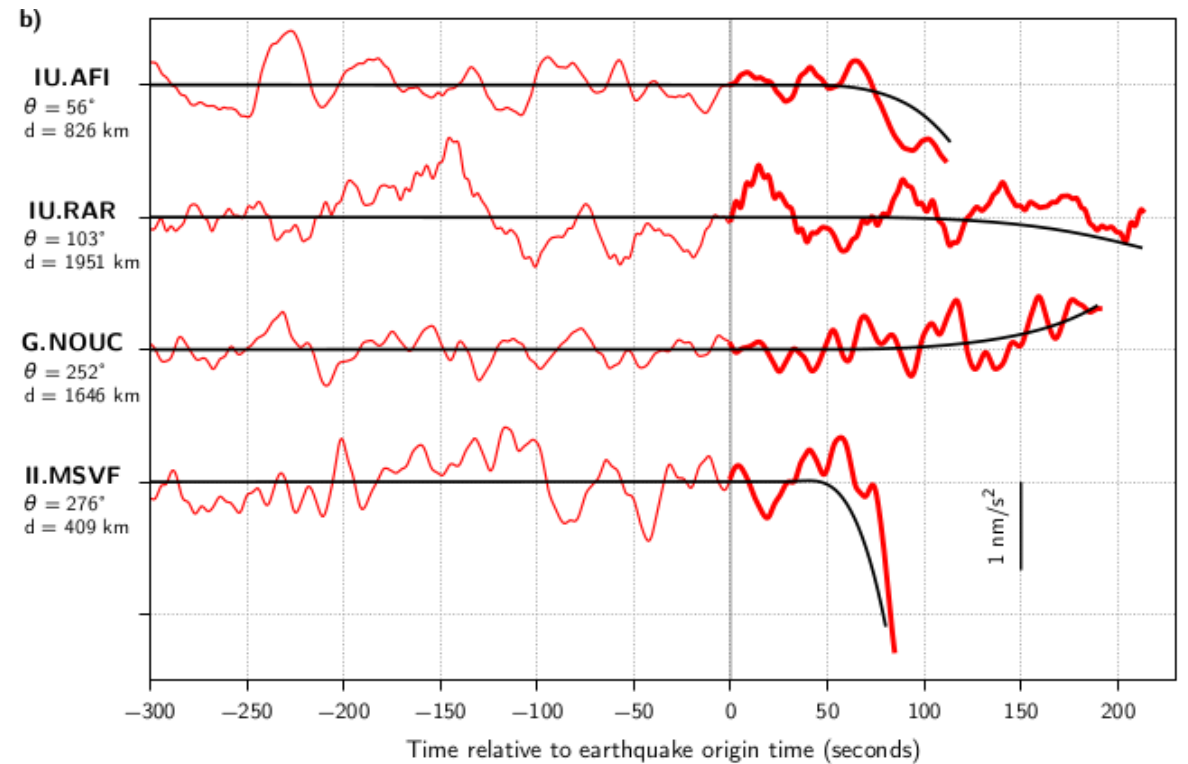
- Large positive signals observed at IPM and PSI
- Good agreement between observed and modeled PEGS

The 2018/08/19 Mw=8.2 deep Fiji earthquake

Map showing the PEGS predicted amplitude (using GCMT source parameters), and the 4 broadband stations with lowest noise in the [0.002-0.03Hz] frequency range



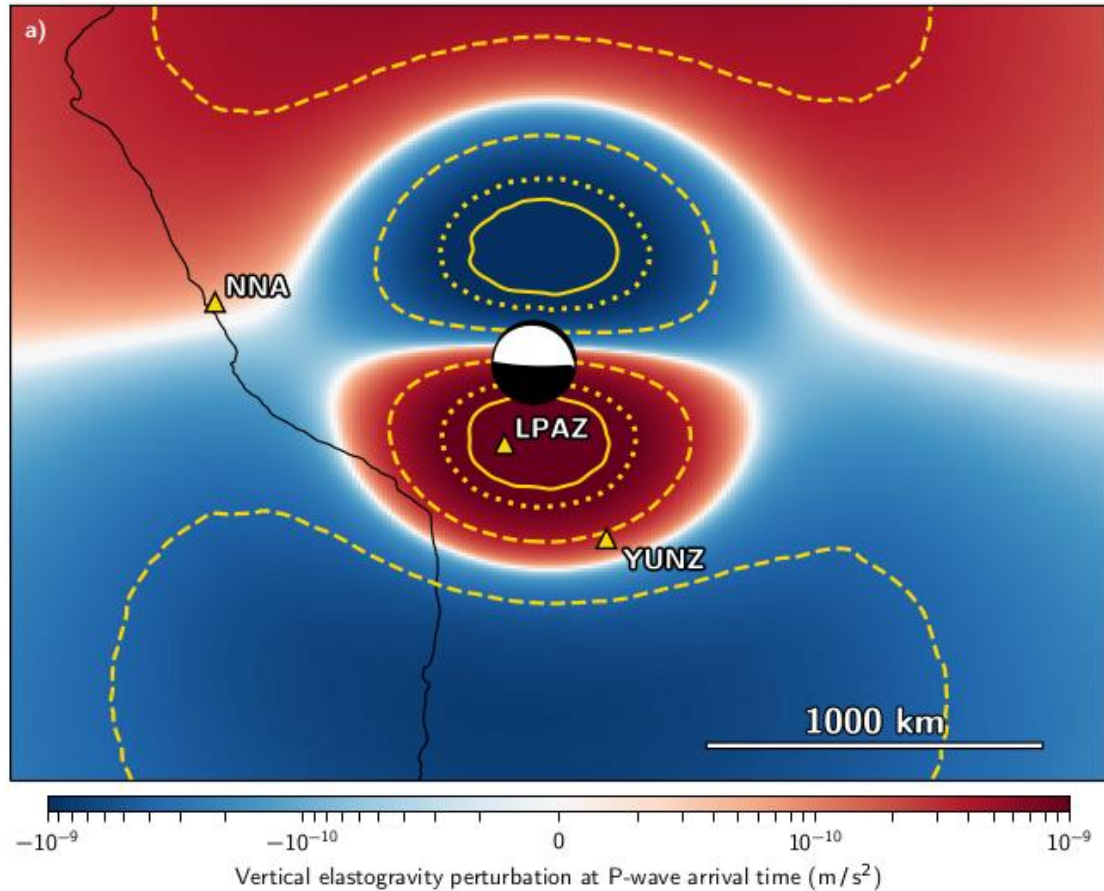
Observed (red) and modeled (black) waveforms at the 4 best stations, using an event-specific source time function (SCARDEC method)



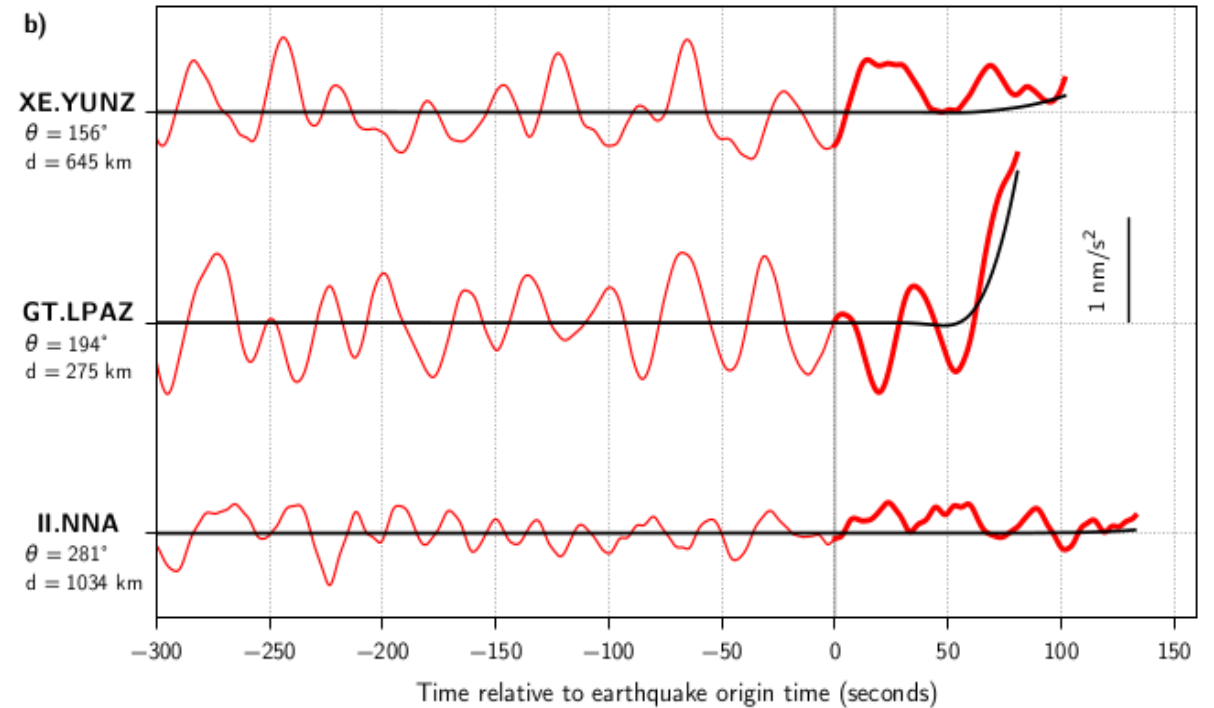
- Large negative signal observed at MSVF (and AFI)
- Positive signal at NOUC
- Good agreement between observed and modeled PEGS

The 1994/06/09 Mw=8.2 deep Bolivia earthquake

Map showing the PEGS predicted amplitude (using GCMT source parameters), and the 3 broadband stations with lowest noise in the [0.002-0.03Hz] frequency range



Observed (red) and modeled (black) waveforms at the 3 best stations, using an event-specific source time function (SCARDEC method)



- Large positive signal observed at LPAZ
- Good agreement between observed and modeled PEGS

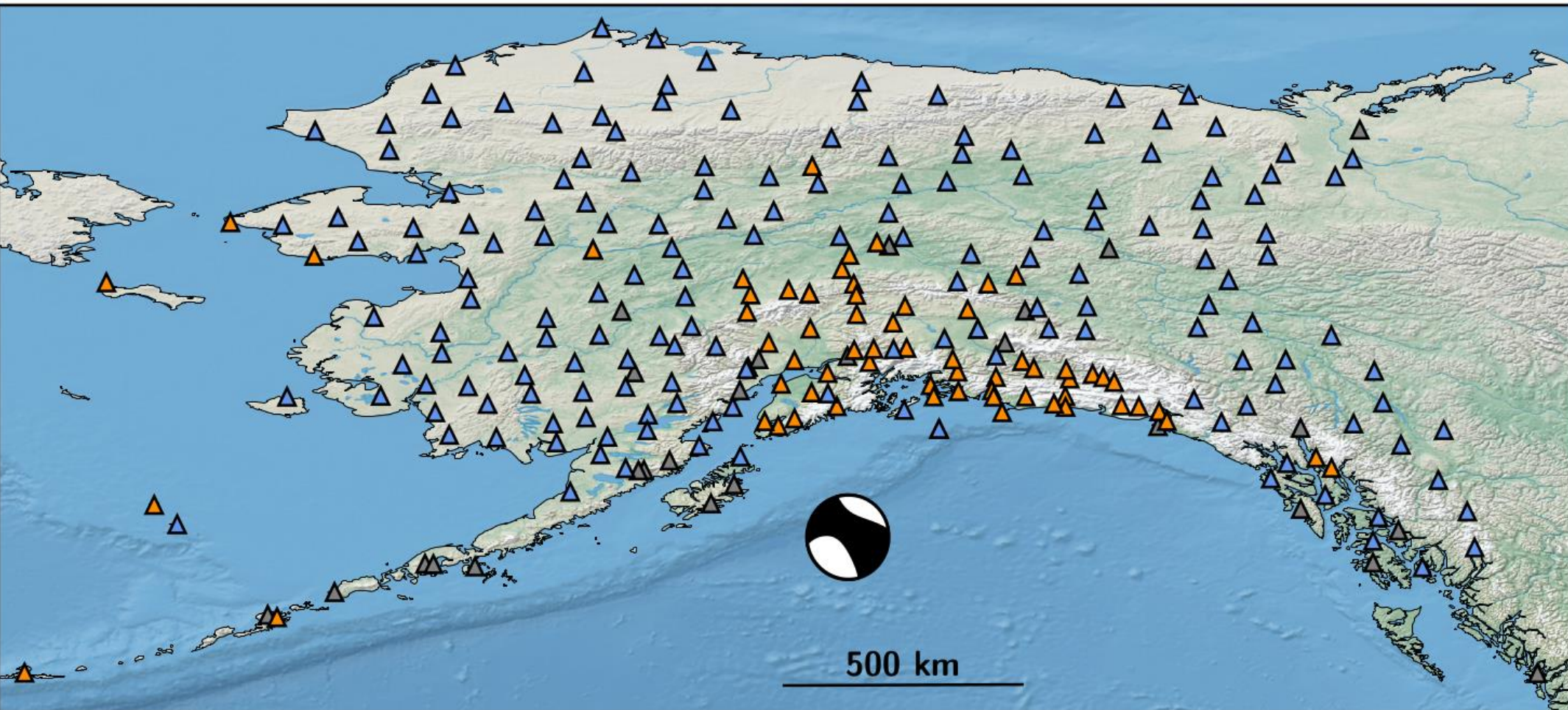
Array observations

The 2018/01/23 Mw=7.9 Gulf of Alaska earthquake

Seismic moment is about 50 times smaller than the Tohoku earthquake, but :

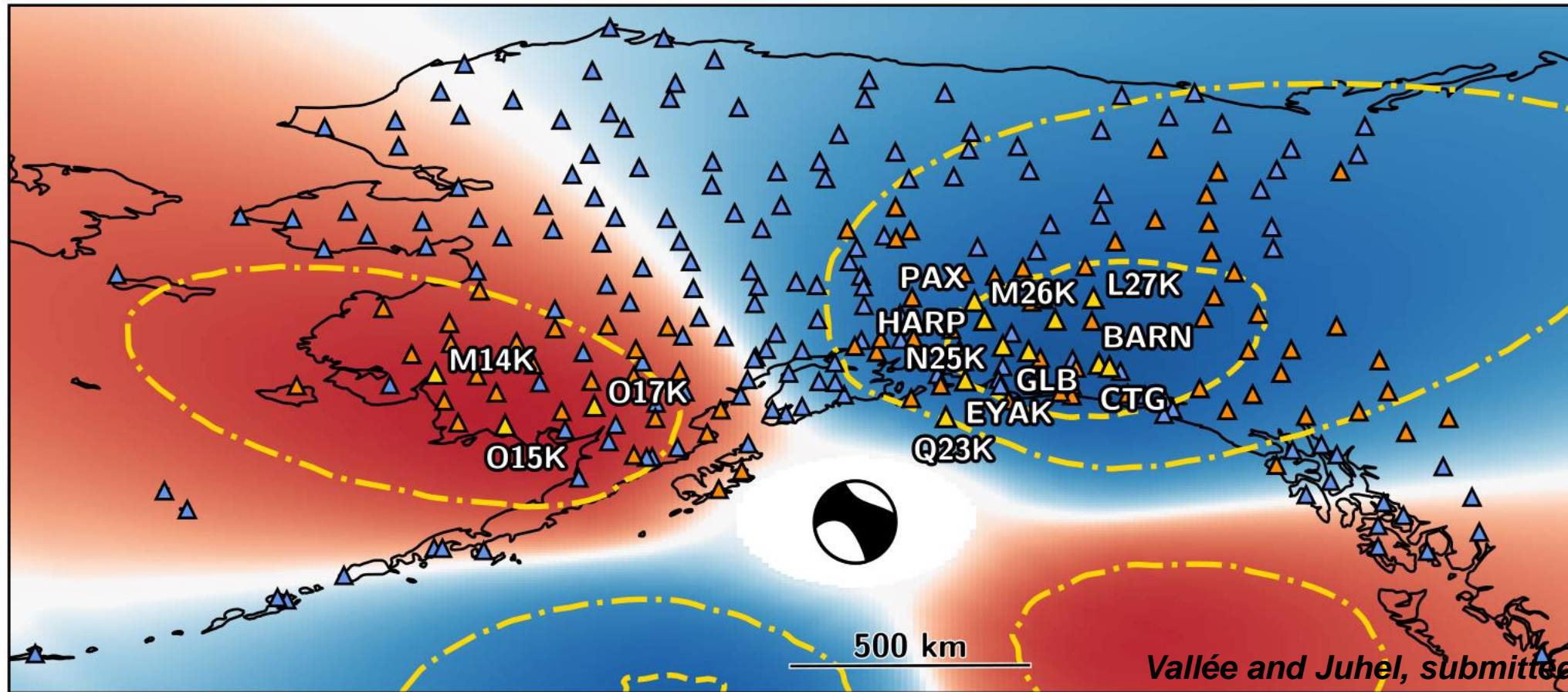
- **Strike-slip mechanism**
- **Excellent coverage provided by USArray (and complemented by the other permanent networks)**

▲ : USArray Transportable Array (TA) ▲ : Alaska Regional Network (AK) ▲ : other networks (AT, AV, US, II, IU, CN)



During the Gulf of Alaska earthquake, ~250 broadband stations in the Alaska region can contribute to the PEGS detection

Predicted PEGS amplitudes

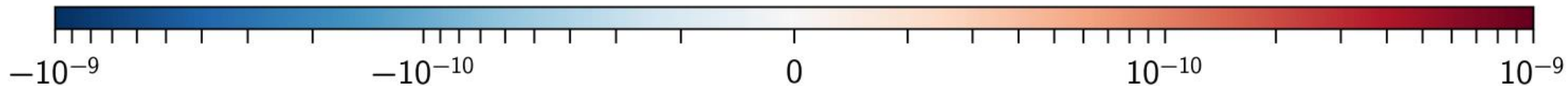


Vertical PEGS
amplitude (at the
P-wave arrival
time)

Dashed-dotted :
+/- 0.2 nm/s²

Dashed :
+/- 0.4 nm/s²

Vallée and Juhel, submitted



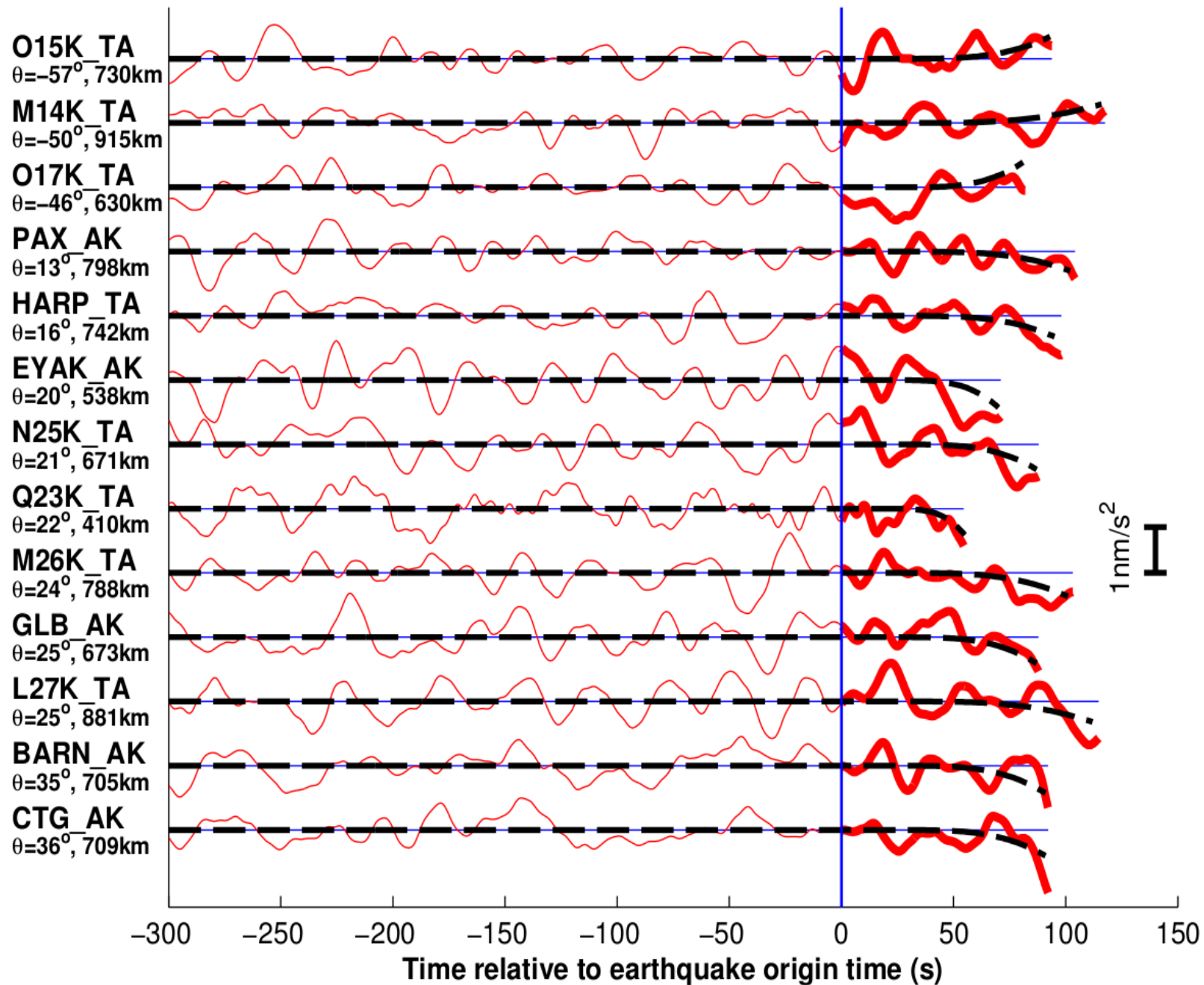
The areas with largest predicted PEGS are well sampled by broadband stations...
But due to the expected amplitudes (max ~ 0.5 nm/s²), direct detection is unlikely

A sensor i has a **good detection potential** if :

- At this location, the **expected PEGS is large**
[quantified by the value of $s_i(T_i^P)$,
expected amplitude at the P-wave arrival
time T_i^P]
- The **instrumental/physical noise is low**
[quantified by the signal variance in the
pre-event period σ_i^2]

We show on the right the **13 best sensors in terms of detection potential**, i.e. the 13 first sensors when ordered by **decreasing order of the coefficient** $\left| \frac{s_i(T_i^P)}{\sigma_i^2} \right|$

Single-station observations **are not sufficient for PEGS detection**



Strategy for array stacking

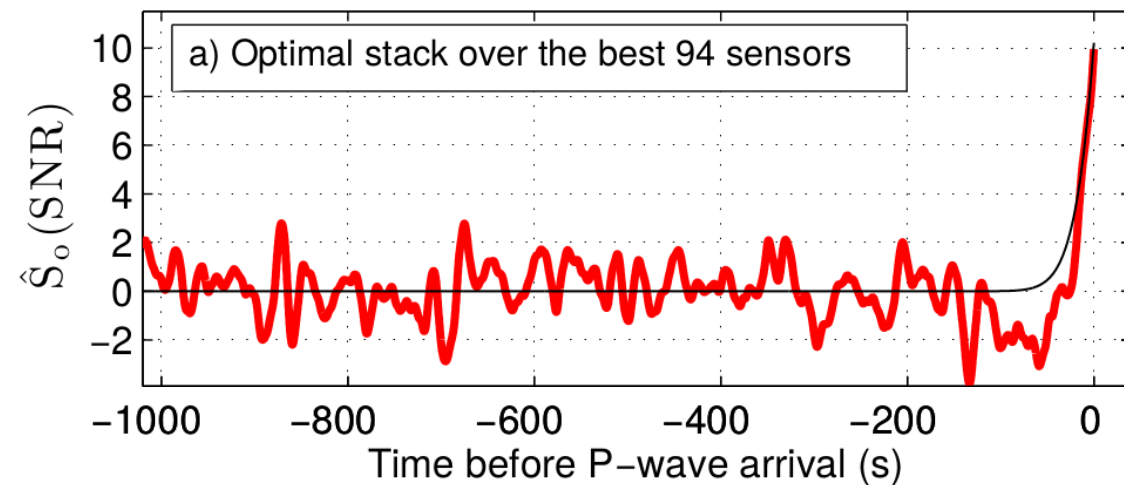
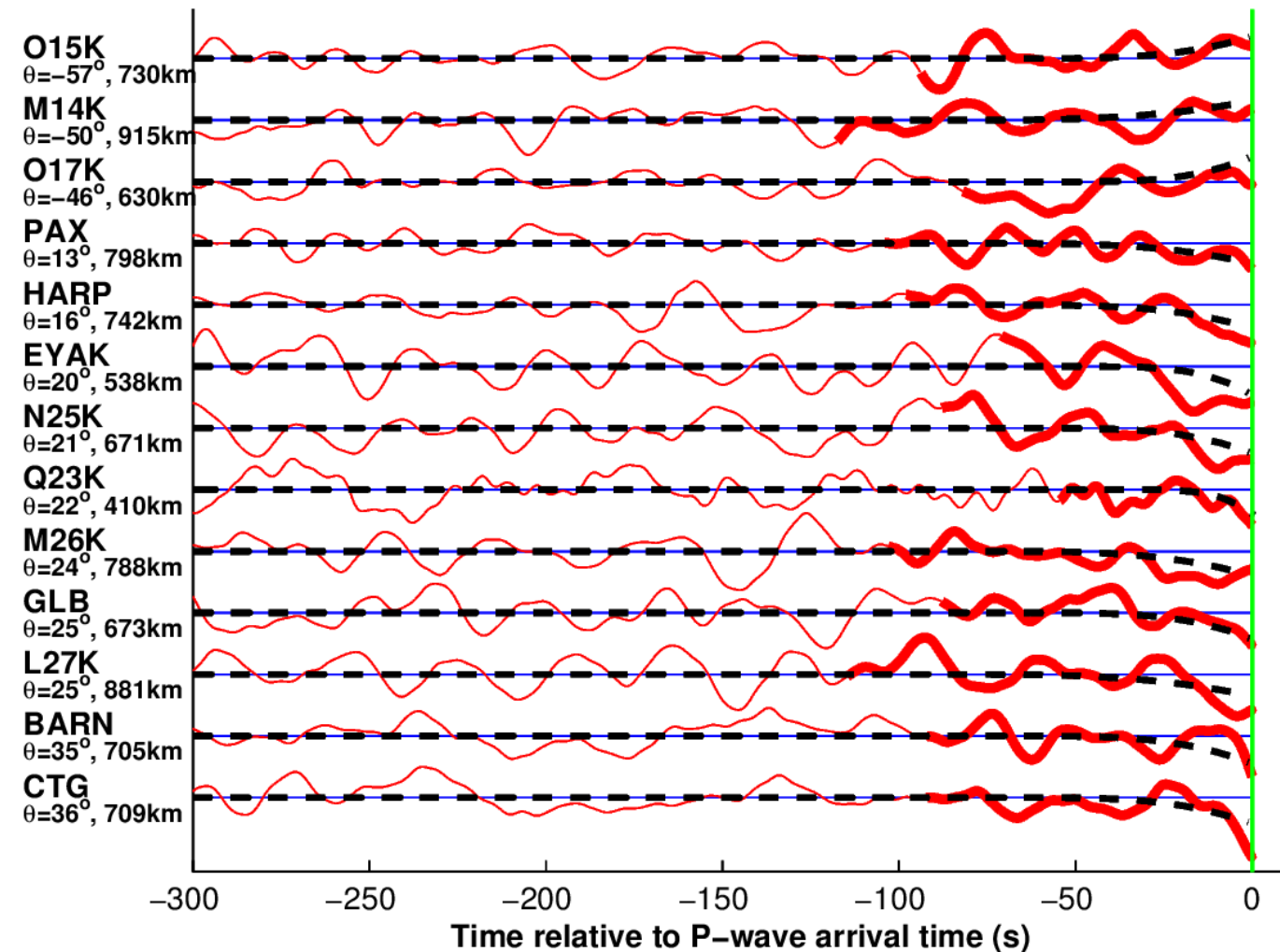
- 1) **Change the reference time of the waveforms a_i from absolute time to P-wave reference time**
(as maximum expected amplitudes occur at the P-wave arrival)

- 2) **Optimal stack, with weights equal to $\frac{s_i(T_i^P)}{\sigma_i^2}$:**

$$S_o(t) = \sum_{i=1}^N \frac{s_i(T_i^P)}{\sigma_i^2} a_i(t + T_i^P)$$

Assumes noise to be Gaussian and stationary
[Tyapkin and Ursin, 2005; Robinson, 1970]

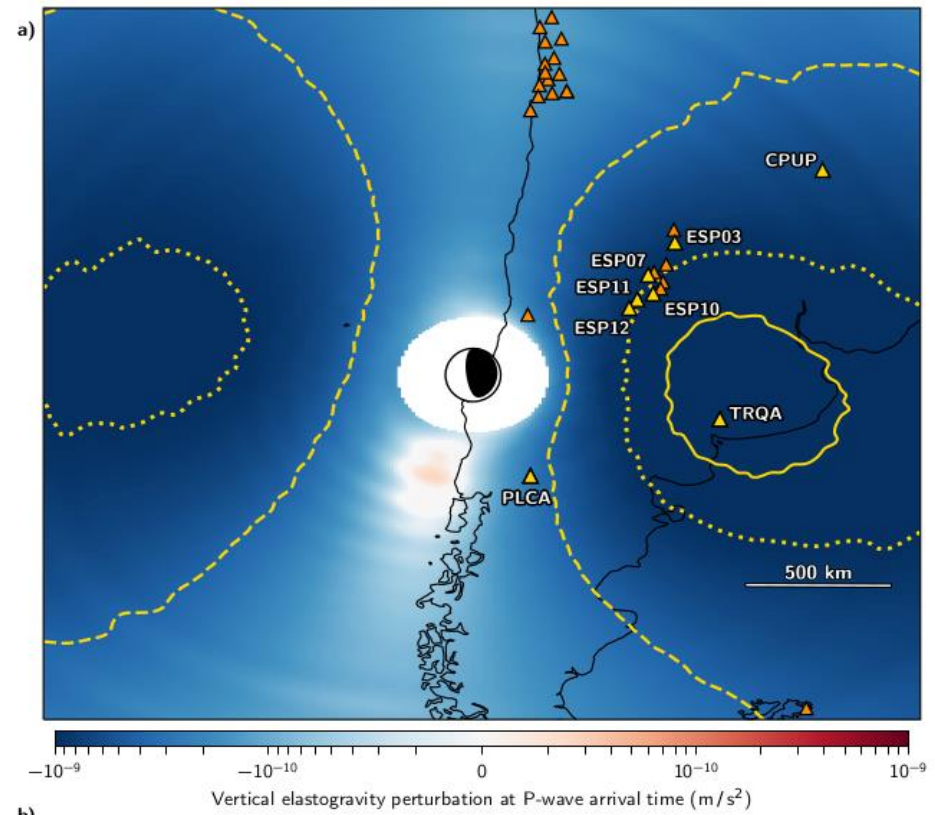
- 3) **Normalization to the the pre-event noise (-> SNR)**



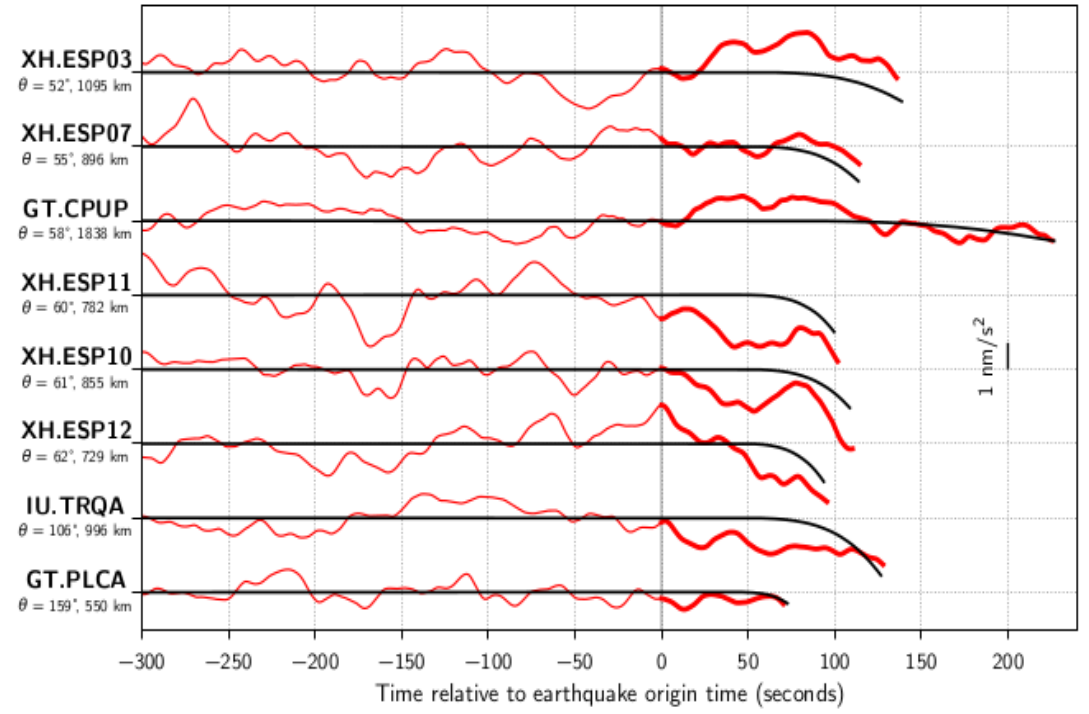
PEGS are detected with a high Signal to noise ratio (~10)

The 2010/02/27 Mw=8.8 Maule (Chile) earthquake

Predicted PEGS amplitudes



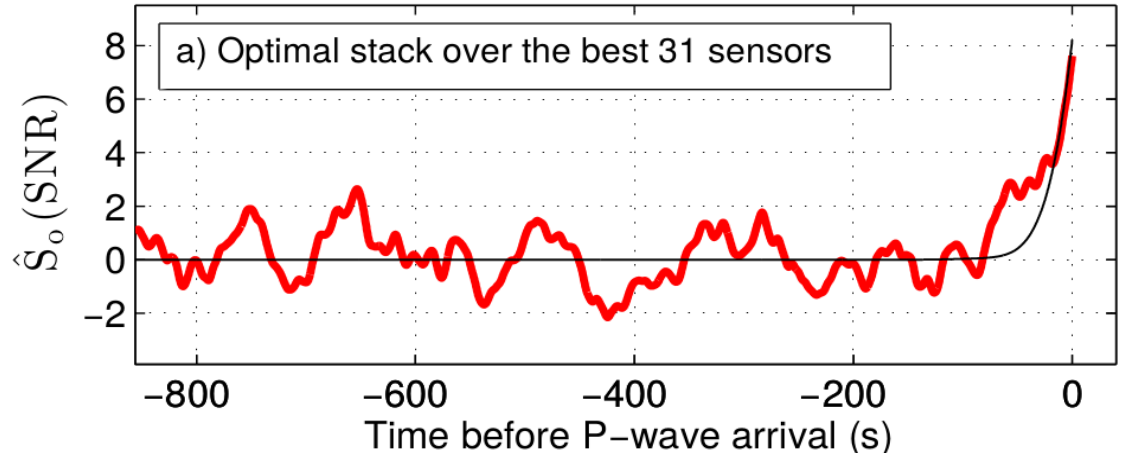
Observed (red) and modeled (black) waveforms at the best located and best quality sensors. Sensor quality is affected by a Mw7 earthquake, 10 hours before in Japan



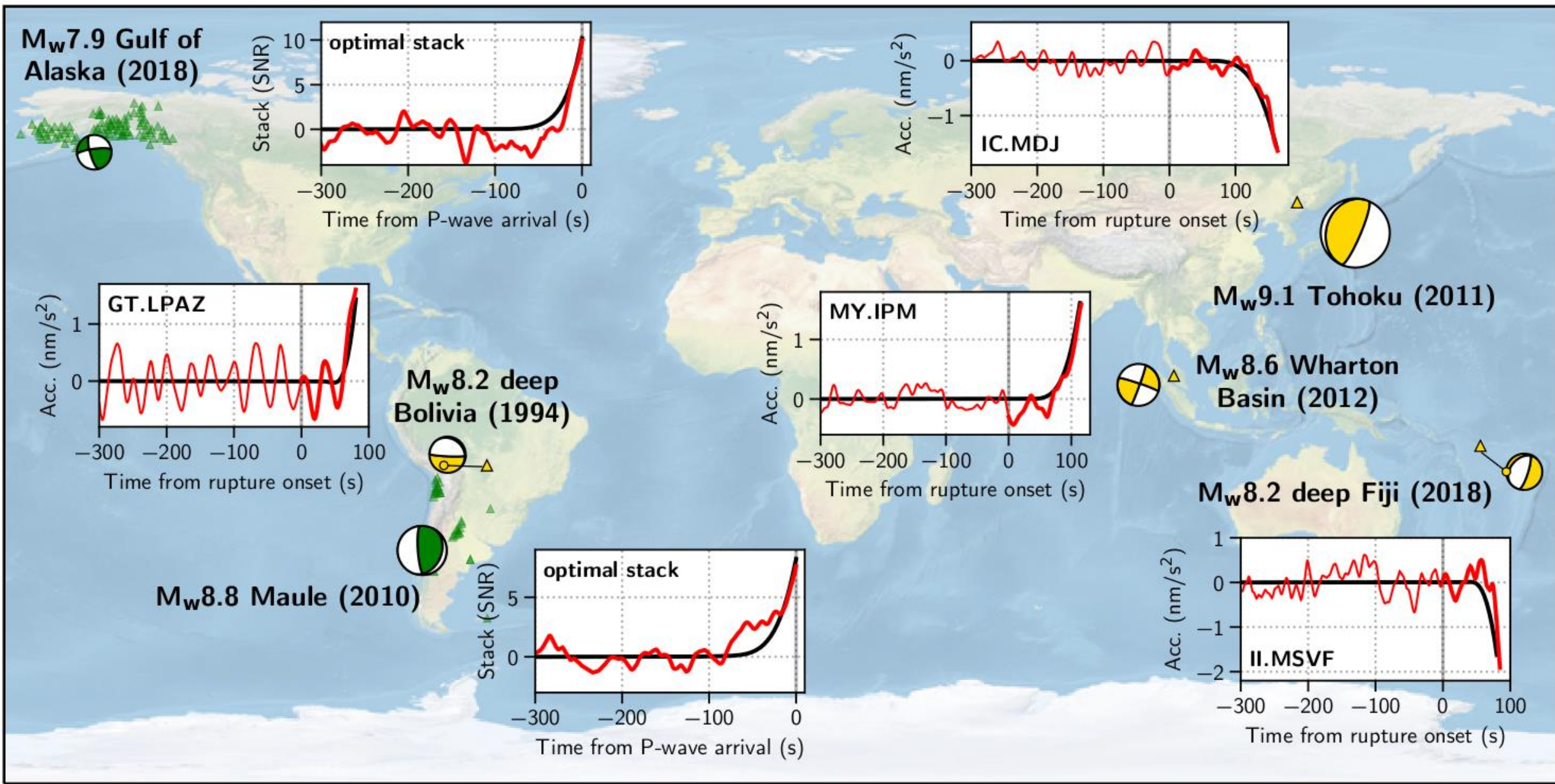
Waveform stack, in P-wave arrival reference-time, weighted by sensor quality and expected amplitude



PEGS are detected with a high Signal to noise ratio (~7.6)



Summary of the PEGS observations to date



Discussion and perspectives

- In addition to the 2011 Tohoku earthquake, we show 5 earthquakes in the [7.9-8.8] magnitude range with unambiguous PEGS observations
- For **earthquake types generating efficient PEGS** (strike-slip or deep-focus, rapidly growing source time function) and **recorded in favorable configurations**, **PEGS can be observed for magnitudes lower than 8**
- Based on their **sensitivity to key source parameters** (magnitude, focal mechanism, source time function), the use of **PEGS can become a new powerful tool for earthquake monitoring and anticipated tsunami alert.**
- In well-instrumented areas with large earthquake hazard (e.g. Alaska, Japan, Cascadia), such approaches can today be tested without additional sensor installation